Am J Transl Res 2021;13(4):2784-2793
www.ajtr.org /ISSN:1943-8141/AJTR0126695

Original Article

The effect of miR-21-5p on the MAP2K3 expressions and cellular apoptosis in the lung tissues of neonatal rats with hyperoxia-induced lung injuries

Anlong Qi[1,2], Tong Wang[3], Wang Li[3], Yongtao Wang[1], Yanfen Chai[1]

[1]Department of Emergency Medicine, Tianjin Medical University General Hospital, Tianjin City, China; [2]Tianjin Medical University, Tianjin City, China; [3]NHC Key Laboratory of Hormones and Development (Tianjin Medical University), Tianjin Key Laboratory of Metabolic Diseases, Tianjin Medical University Chu Hsien-I Memorial Hospital & Tianjin Institute of Endocrinology, Tianjin City, China

Received November 20, 2020; Accepted December 20, 2020; Epub April 15, 2021; Published April 30, 2021

Abstract: Objective: To explore the effect of miR-21-5p on the MAP2K3 expressions and cellular apoptosis in the lung tissues of neonatal rats with hyperoxia-induced lung injuries (HILI). Methods: Twenty Sprague-Dawley neonatal rats were assigned to the normal group, and 120 rats were used to create a HILI model and were divided into the following six groups of 20 rats each: the model group, the miR-21-5p NC group, the miR-21-5p agomir group, the oe-NC group (MAP2K3 overexpression NC), the oe-MAP2K3 group, and the miR-21-5p agomir+oe-MAP2K3 group. Results: miR-21-5p can target MAP2K3. Compared with the normal rats, the rats with HILI had lower miR-21-5p expression levels and higher MAP2K3 expression levels in the lung tissues (both $P<0.05$). Unlike the normal group, the other groups all presented different degrees of lung injuries, lower Bcl-2 expression levels, higher cellular apoptosis rates, and higher expression levels of cleaved caspase-3, Bax, IL-6, and TNF-α (all $P<0.05$). Compared with the model and the miR-21-5p NC groups, the miR-21-5p agomir group had better results in terms of the aforementioned markers; compared with the oe-NC group, the oe-MAP2K3 group had worse results in terms of these markers (all $P<0.05$). Moreover, we found that the protective effects of miR-21-5p overexpression on the lung tissues of HILI rats can be partially blocked by MAP2K3 overexpression. Conclusion: miR-21-5p can inhibit MAP2K3 expression and reduce cellular apoptosis in HILI, thereby exerting protective effects on neonatal rats with HILI.

Keywords: Apoptosis, hyperoxia-induced lung injuries, MAP2K3, miR-21-5p, neonatal rats

Introduction

Hyperoxia-induced lung injuries (HILI) are caused by a prolonged inhalation of high concentrations of oxygen. The disease can lead to pulmonary hypoplasia or even death in newborn babies [1-3]. So far, the pathogenesis of HILI has not been fully elucidated, and there is a lack of effective therapies for HILI [4, 5]. Therefore, it is essential to investigate the mechanism of HILI in order to find useful methods for treating infants with HILI.

The apoptosis of lung alveolar epithelial cells has been widely recognized as the major cause of the occurrence and development of HILI. Some studies reported that the miR-21-5p levels decrease substantially in the lung alveolar epithelium during HILI, showing that miR-21-5p may participate in the apoptosis of the lung alveolar epithelial cells [6]. microRNAs (miRNAs), which can regulate cell proliferation and apoptosis by targeting the downstream genes and regulating the expressions of the target genes after transcription, have become a popular research topic in recent years [7-10]. We suspected that there may be downstream target genes of miR-21-5p in HILI. After searching a bioinformatics website, we determined that mitogen-activated protein kinase kinase 3 (MAP2K3) is a possible target of miR-21-5p. MAP2K3 belongs to the family of mitogen-activated protein kinases (MAPK) and is an upstream activator of p38 MAPK [11-14]. Currently, the detailed mechanism of how MAP2K3 acts in HILI remains unclear. However,

some researchers have documented that the MAPK signaling pathway is related to oxidative stress injuries in various diseases including HILI [15, 16]. Thus, we speculated that miR-21-5p may affect pulmonary cell apoptosis via regulating MAP2K3 expression in HILI, thereby influencing the development of this disease.

In this study, we explored the targeting relationship between miR-21-5p and MAP2K3 and the effects of miR-21-5p and MAP2K3 on the neonatal rat model of HILI.

Materials and methods

Animal subjects

Healthy specific pathogen-free Sprague-Dawley neonatal rats were used in this study (supplier: Guangdong Medical Laboratory Animal Center, China). The rats were raised at 22°C under 60% humidity and a 12 h light: dark cycle. All the rats were fed a normal diet. Approval for this experiment was obtained from the Ethics Committee of Tianjin Medical University General Hospital.

Model establishment and grouping

One-hundred and forty neonatal rats were used in this study. Of them, 20 were assigned to the normal group (the normal rats), and the rest were used to create the HILI disease model and were randomized into six groups of 20 rats each: the model group, the miR-21-5p NC group (a miR-21-5p negative control), the miR-21-5p agomir group (miR-21-5p overexpression), the oe-NC group (a negative control for MAP2K3 overexpression), the oe-MAP2K3 group (MAP2K3 overexpression), and the miR-21-5p agomir+oe-MAP2K3 group (overexpression of both miR-21-5p and MAP2K3). The miR-21-5p NC, miR-21-5p agomir, oe-NC, and oe-MAP2K3 were purchased from Meixuan Biological Science and Technology, Shanghai, China.

The rats in the normal group were raised in an environment of normal oxygen concentration and were fed with breast milk. The rats in the other groups were raised in an environment of 80% oxygen concentration and were freed from this environment for 1 h per day to receive food and water. The air pumps in the rats' chambers were replaced every 24 h to avoid oxygen poisoning. Intraperitoneal injections of the corresponding agents (500 μg/kg) were given to the rats in each group once a day for seven days in their chambers [17]. After the treatment, the lung tissues and the bronchoalveolar lavage fluid (BALF) were collected from the rats.

Dual-luciferase reporter (DLR) assay

By using the bioinformatics tool (www.targetscan.org), we found the pairing of miR-21-5p with MAP2K3 in rats. The pGL3-MAP2K3 mut, pGL3-MAP2K3 wt, miR-21-5p NC, and miR-21-5p agomir vectors were constructed by Hanbio, Shanghai, China. The pGL3-MAP2K3 mut or pGL3-MAP2K3 wt vectors were transfected into the 293T cells with miR-21-5p NC or miR-21-5p agomir. After 24 h of transfection, the cells were lysed using a DLR assay kit (E2920, Promega, USA) and centrifuged at 12,000 g for 1 min to collect the supernatant for the fluorescence analysis. The experiment was conducted in the dark. Relative luciferase activity = firefly luciferase activity/renilla luciferase activity.

Hematoxylin and eosin (H&E) staining

We used H&E staining to examine the pathological changes in the lung tissues of the rats. Five specimens were collected from each group. The samples were routinely fixed, dehydrated, embedded, and sectioned. The sections were then dewaxed, hydrated, treated with 1% hydrochloric acid alcohol for 10 s and stained with eosin for 1 min. Finally, the sections were then dehydrated through a gradient of alcohol, cleared in xylene (Solarbio, Beijing, China), mounted in neutral balsam, and placed under a lighted microscope (XP-330, Bingyu Optical Instrument, Shanghai, China) to examine the pathological changes.

TUNEL staining

Five paraffin sections of the lung tissues were collected from each group. The samples were treated with phosphate-buffered saline (PBS) containing 2% H_2O_2 at 37°C for 5 min followed by two washes in PBS (5 min per wash). After removing the excess solution, the sections were treated with a terminal deoxynucleotidyl transferase (TdT) buffer (Merck, USA) at 37°C for 5 min. Next, the sections were treated with 54 μL of TdT reagent (Merck, USA) in a humidified box for 1 h followed by three washes in PBS (5 min per wash). The samples were then incu-

Table 1. Primer sequences

Gene	Primer sequences (5'-3')
miR-21-5p	F: GGGTAGCTTATCAGACTGA
	R: GTGCAGGGTCCGAGGT
MAP2K3	F: ACGGATATCCTGTGTGTCCA
	R: TACCACTCTGAGCATGCCG
Caspase-3	F: CAACAACGAAACCTCCGTGG
	R: ACACAAGCCCATTTCAGGGT
Bax	F: GACACCTGAGCTGACCTTGG
	R: AGTTCATCGCCAATTCGCCT
Bcl-2	F: TTCCTTAGGCGCGGTGAAAC
	R: GACAAGGGAGGCATCTTCGG
U6	F: CGCTTCGGCAGCACATATAC
	R: TTCACGAATTTGCGTGTCAT
GAPDH	F: TGTGAACGGATTTGGCCGTA
	R: GATGGTGATGGGTTTCCCGT

Note: F: forward. R: reverse. MAP2K3: mitogen-activated protein kinase kinase 3.

bated with peroxidase-labelled digoxin antibodies (Abcam, UK) in a humidified box for 30 min followed by four washes in PBS (5 min per wash). Fresh diaminobenzidine (Merck, USA) was added to the samples to develop the color. After 5 min, the sections were washed with distilled water and stained with methyl green (Merck, USA) for 10 min. Next, the sections were washed with distilled water, dehydrated with normal butyl alcohol and xylene, and sealed for observation under a microscope. Five fields were randomly picked on each section to photograph. The ratio of TUNEL positive cells = number of TUNEL positive cells/total cell count * 100%.

ELISA

We measured the interleukin (IL)-6 and tumor necrosis factor (TNF)-α levels in the rats' serum using the ELISA assay. The tests were conducted according to the kit's instructions (IL-6, RAB0311, Merck, NJ, USA; TNF-α, RAB0479, Merck, NJ, USA).

qRT-PCR

Five specimens of the lung tissues from each group (0.01 g) were ground with 500 μL of Trizol (15596-018, Invitrogen, California, USA) to extract the total RNA. The RNAs were then reverse-transcribed to cDNAs according to the manufacturer's instructions (RR037A, TaKaRa, Dalian, China). The cDNAs (2 μl) were diluted 10 times for qPCR. The total reaction volume of qPCR (10 μL) consisted of 2 μL of cDNA, 1 μL of forward primer, 1 μL of reverse primer, 5 μL of SYBR® Premix Ex Taq™ II (2×), and 1 μL of distilled water. qRT-PCR (PCR instrument: Bio-Rad Laboratories, USA) was conducted with the following parameters: 95°C for 5 min (pre-denaturation), 94°C for 30 s (denaturation), 58°C for 30 s (annealing), and 72°C for 30 s (extension). The PCR cycle was repeated 35 times.

We performed the $2^{-\Delta\Delta Ct}$ method to calculate the genes' relative expression levels. U6 was the internal control for miR-21-5p, and GAPDH was the internal control for MAP2K3, cleaved caspase-3, Bax, and Bcl-2. The primers were synthesized by Wuhan Bojie, China and are displayed in **Table 1**.

Western blot

Five specimens of the lung tissues from each group (0.01 g) were placed in an ice bath to make homogenate and then treated with a protein lysis buffer (Solarbio, Beijing, China) at 4°C for 30 min with agitation once every 10 min. Next, the samples were centrifuged for 2 min at 10,000×g at 4°C to obtain the supernatant. The protein concentration of the supernatant was measured using a BCA kit (20201ES76, Yeasen, Shanghai, China). Next, 20 μL of samples were equally uploaded to each lane for electrophoresis (10% separating gel and 4% stacking gel). After SDS-PAGE, the proteins were transferred to nitrocellulose membranes. The membranes were sealed in 5% skim milk (Ybio, Shanghai, China) at 4°C overnight and incubated with diluted polyclonal primary antibodies of rabbit anti-MAP2K3 (ab95037, Abcam, USA), anti-cleaved caspase-3 (ab49822, Abcam, USA), Bax (ab53154, Abcam, USA), anti-Bcl-2 (ab196495, Abcam, USA), and anti-GAPDH (ab181602, Abcam USA) at 4°C overnight. Afterward, the membrane was washed in PBS three times at room temperature (5 min per wash) and treated with horseradish peroxidase-conjugated goat anti-rabbit IgG secondary antibody (ab150077, Abcam, USA) under agitation at 37°C for 1 h. The membrane was then washed in PBS at room temperature three times (5 min per wash) and immersed in ECL (Pierce, MA, USA) at room temperature for 1 min. After removing the

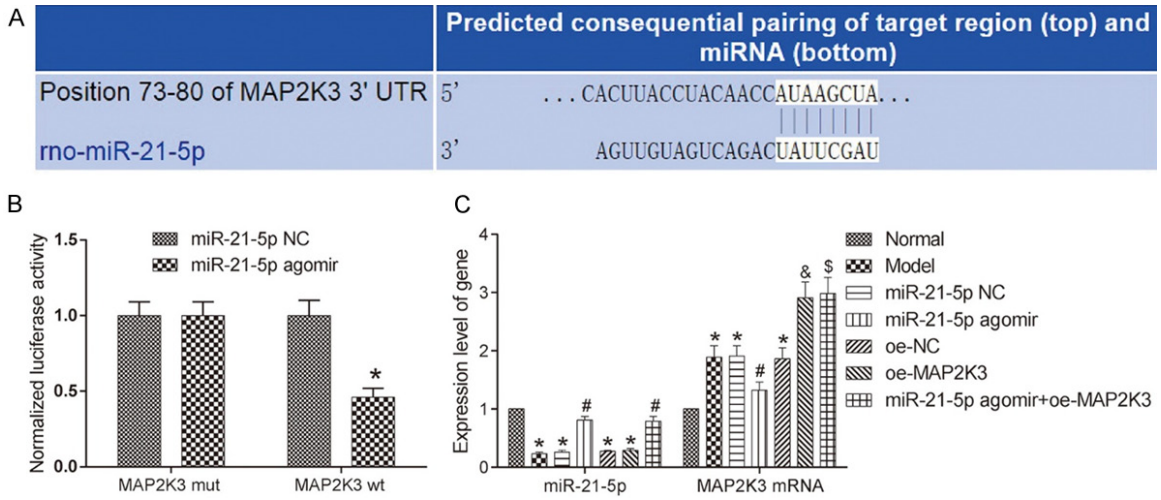

Figure 1. miR-21-5p can target MAP2K3 and inhibit its expression. A: The pairing of miR-21-5p with MAP2K3 as predicted by the bioinformatics website; B: miR-21-5p can target MAP2K3 as verified by dual-luciferase reporter assay. Compared with the miR-21-5p NC group, *P<0.05. C: The expressions of miR-21-5p and MAP2K3 in the lung tissues of each group determined by qRT-PCR. Compared with the normal group, *P<0.05; compared with the miR-21-5p NC group; #P<0.05; compared with the oe-NC group, &P<0.05; compared with the miR-21-5p agomir group, $P<0.05. MAP2K3: mitogen-activated protein kinase kinase 3.

excess liquid, the membrane was wrapped with plastic wrap and placed in the dark for an X-ray film exposure and developing to capture the image. The relative protein expression level was the ratio of the grayscale value of the target band to the grayscale value of the internal control band.

Statistical analysis

SPSS 21.0 (SPSS Inc., USA) was used for the data analysis. The measurement data are presented as the mean ± standard deviation. Independent samples t-tests were conducted for the comparisons between two groups; multiple groups were compared using one-way analyses of variance and Bonferroni post-hoc tests. P<0.05 represented statistical significance.

Results

MiR-21-5p can target MAP2K3 and inhibit its expression

The bioinformatics website predicted the existence of a miR-21-5p binding site on MAP2K3 (**Figure 1A**). To further verify this relationship, we conducted a DLR assay and found that the luciferase activity of the cells transfected with the miR-21-5p agomir and the MAP2K3 wt were much lower than the cells transfected with miR-21-5p NC, indicating miR-21-5p can target MAP2K3. Meanwhile, qRT-PCR and Western blot were conducted to measure the miR-21-5p and MAP2K3 expressions in the rats' lung tissues. Compared with the normal group, the other groups had lower expression levels of miR-21-5p and higher mRNA and protein expression levels of MAP2K3 (all P<0.05). The expression levels of miR-21-5p and MAP2K3 in the miR-21-5p NC and oe-NC groups were similar to those in the model group. The miR-21-5p agomir group had a higher miR-21-5p expression level and a lower MAP2K3 mRNA expression level than the miR-21-5p NC group (both P<0.05). Compared with the oe-NC group, the oe-MAP2K3 group had a similar miR-21-5p level (P>0.05) and a higher MAP2K3 mRNA level (P<0.05). The findings indicate that miR-21-5p can target MAP2K3 and inhibit its expression in neonatal rats. See **Figure 1**.

Pathological changes in each group

H&E staining was performed to examine the pathological changes in the lung tissues of each group. The normal group presented clear pulmonary alveolus structures and a normal thickness of the lung interstitium, but the other groups exhibited different degrees of pathological changes, including a thinning of the lung interstitium and a swelling of the pulmonary

alveolus. To further assess the pathological conditions, we calculated the wet-to-dry (W/D) lung weight ratio and found that compared with the normal group, the other groups had higher levels of W/D weight ratio (all P<0.05). The miR-21-5p NC group and the oe-NC group had similar W/D weight ratio levels compared to the model group (both P>0.05). The W/D lung weight ratio in the miR-21-5p agomir group was lower than it was in the miR-21-5p NC and the miR-21-5p agomir+oe-MAP2K3 groups; the W/D lung weight ratio in the oe-MAP2K3 group was higher than it was in the oe-NC group (all P<0.05). These findings reveal that HILI can be ameliorated by miR-21-5p overexpression and aggravated by MAP2K3 overexpression, and MAP2K3 overexpression can hinder the repairing effect of miR-21-5p overexpression on lung injuries. See **Figure 2**.

Cellular apoptosis in each group

Since HILI is accompanied by pulmonary cell apoptosis in the neonatal rats, TUNEL staining was conducted to measure the cellular apoptosis in the lung tissues of each group. Unlike the normal group, the other groups had higher apoptotic rates (all P<0.05). Both the miR-21-5p NC and oe-NC groups had cell apoptotic rates similar to the model group (both P>0.05). The cell apoptotic rate in the miR-21-5p agomir group was lower than it was in the miR-21-5p NC and miR-21-5p agomir+oe-MAP2K3 groups (both P<0.05). The apoptotic rate in the oe-MAP2K3 group was higher than it was in the oe-NC group (P<0.05). Meanwhile, the mRNA expressions of caspase-3, Bax, and Bcl-2, and the protein expressions of cleaved caspase-3, Bax, and Bcl-2 were measured using qRT-PCR and Western blot, respectively. Compared with the normal group, the other groups had higher levels of caspase-3, cleaved caspase-3, and Bax and lower levels of Bcl-2 (all P<0.05). Both miR-21-5p NC and oe-NC groups had similar levels of these markers as compared to the model group (all P>0.05). The miR-21-5p agomir group had lower levels of caspase-3, cleaved caspase-3, and Bax and higher level of Bcl-2 than the miR-21-5p NC and the miR-21-5p agomir+oe-MAP2K3 groups; the oe-MAP2K3 group had higher levels of caspase-3, cleaved caspase-3, and Bax and lower levels of Bcl-2 than the oe-NC group (all P<0.05). These results reveal that cellular apoptosis can be inhibited by miR-21-5p overexpression and promoted by MAP2K3 overexpression. See **Figure 3**.

The inflammatory factor levels in each group

ELISA was conducted to measure the IL-6 and TNF-α levels in the rats' BALF. Unlike the normal group, the other groups had higher TNF-α and IL-6 levels (all P<0.05). Both the miR-21-5p NC and oe-NC groups had similar levels of TNF-α and IL-6 compared to the model group (all P>0.05). The IL-6 and TNF-α levels in the miR-21-5p agomir group were lower than the levels in the miR-21-5p NC and the miR-21-5p agomir+oe-MAP2K3 groups; the IL-6 and TNF-α levels in the oe-MAP2K3 group were higher than they were in the oe-NC group (all P<0.05). These findings indicate that the pulmonary inflammatory response can be inhibited by miR-21-5p overexpression and promoted by MAP2K3 overexpression. See **Figure 4**.

Discussion

Normal oxygen concentration is necessary for human body to maintain normal life activities, but a high concentration of oxygen can damage the body, and a prolonged exposure to a high oxygen concentration can cause HILI [18-20]. So far, there are still no effective preventive and treatment methods for HILI. Thus, it is essential to investigate the mechanism of HILI to provide a theoretical basis for the clinical prevention and treatment of this disease.

HILI is characterized by the apoptosis of lung alveolar epithelia and the inflammatory progression [21]. The occurrence and development of inflammation has an essential role in the pathogenesis of HILI. During the early stage of HILI, the up-regulation of MMP-8 expression can cause injury in the capillary walls of the pulmonary alveolus, thus increasing the exudation in the pulmonary alveolus and the development of the inflammatory response [22, 23]. The inflammatory response is usually accompanied by the release of the inflammatory factors including TNF-α and IL-6, while the release and accumulation of these factors in the pulmonary alveolus can further aggravate lung injuries [24, 25]. The apoptosis of the lung alveolar epithelia is a key element of lung injuries. Bcl-2 family members participate in the complicated apoptotic mechanism in HILI. The Bcl-2 family

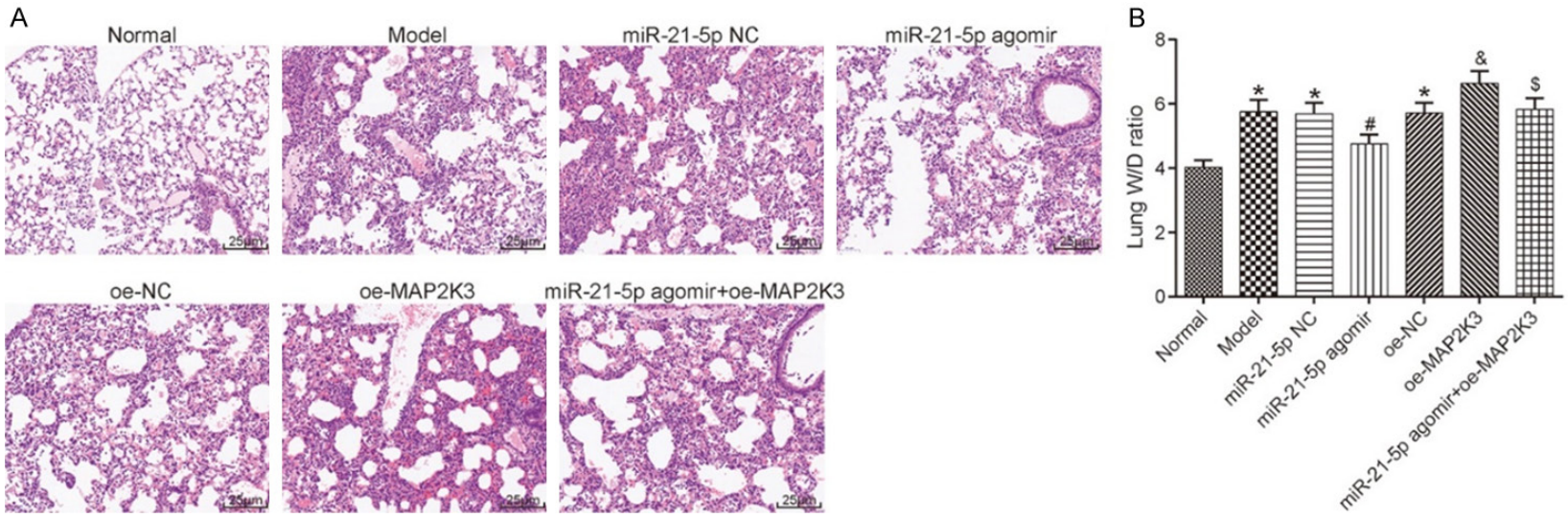

Figure 2. H&E staining results and W/D lung weight ratio in the lung tissues of each group. A: H&E staining results (200×); B: W/D weight ratio in the lung tissues of each group. Compared with the normal group, $^{*}P<0.05$, compared with the miR-21-5p NC group, $^{\#}P<0.05$; compared with the oe-NC group, $^{\&}P<0.05$; compared with the miR-21-5p agomir group, $^{\$}P<0.05$. H&E: hematoxylin and eosin; W/D: wet-to-dry; MAP2K3: mitogen-activated protein kinase kinase 3.

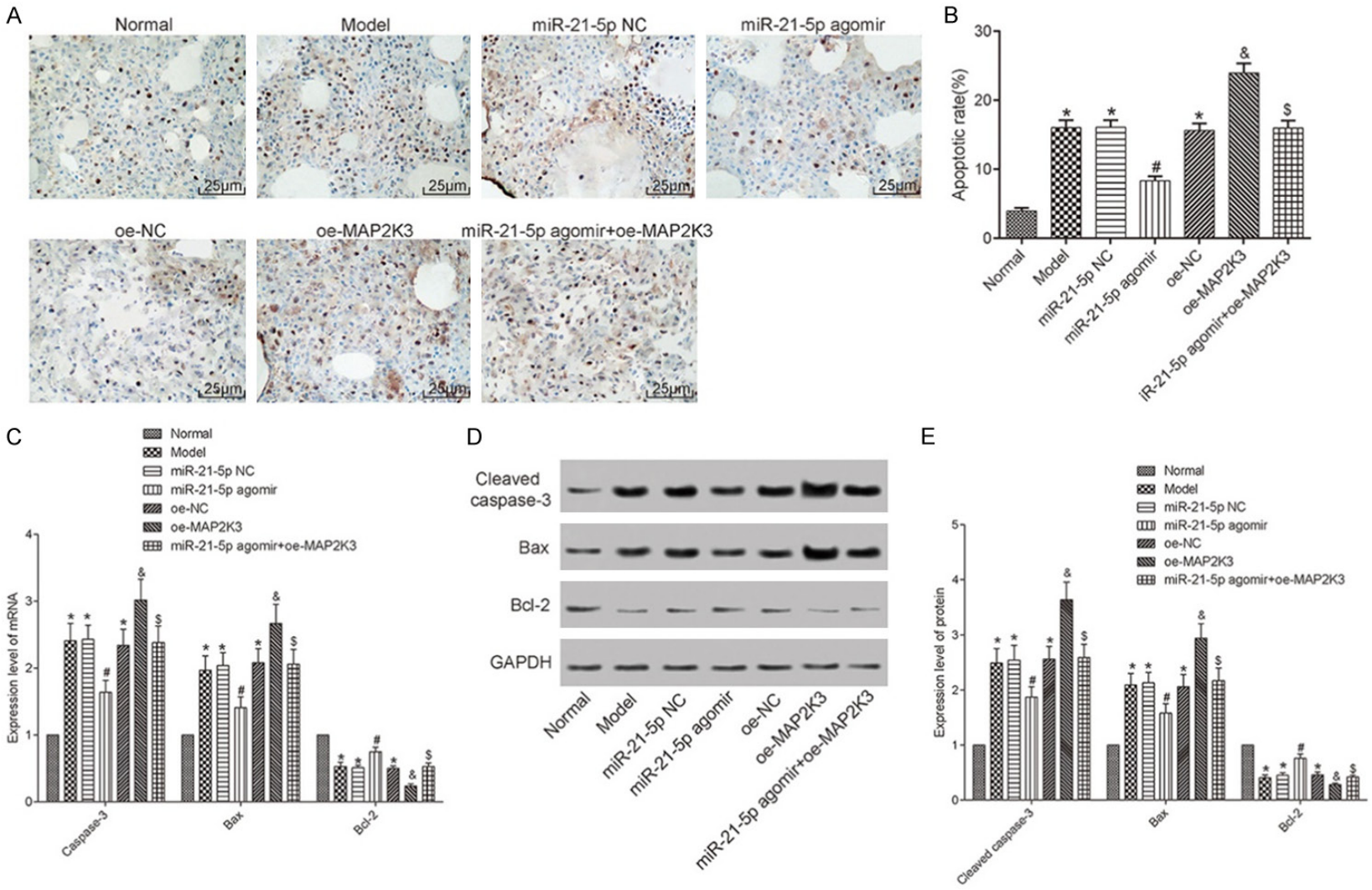

Figure 3. The cellular apoptosis in each group. A: TUNEL staining results (200×); B: The pulmonary apoptotic rate in each group; C: The mRNA expression levels of the apoptosis-associated factors measured with qRT-PCR; D: Image of the Western blot results; E: The protein expression levels measured using Western blot. Compared with the normal group, $^{*}P<0.05$; compared with the miR-21-5p NC group, $^{\#}P<0.05$; compared with the miR-21-5p agomir group, $^{\&}P<0.05$; compared with the miR-21-5p agomir group, $^{\$}P<0.05$. TUNEL: Terminal deoxynucleotidyl transferase dUTP nick end labeling; MAP2K3: mitogen-activated protein kinase kinase 3.

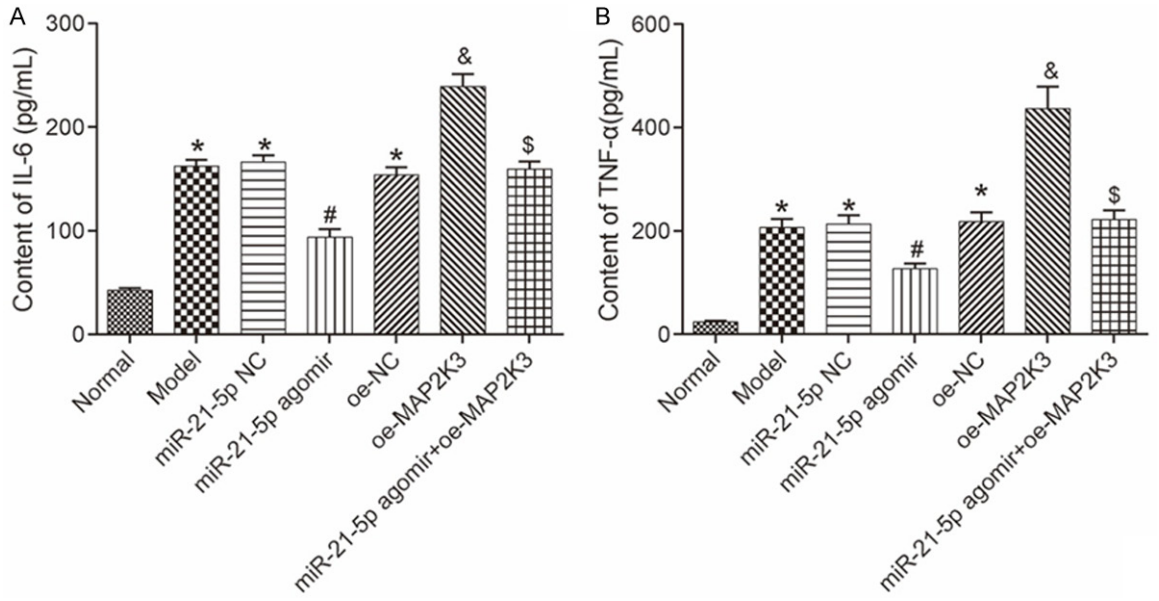

Figure 4. The IL-6 and TNF-α levels in rats' BALF measured using ELISA. A: The IL-6 level in each group; B: The TNF-α level in each group. Compared with the normal group, *P<0.05; compared with the miR-21-5p NC group, #P<0.05; compared with the oe-NC group, &P<0.05; compared with the miR-21-5p agomir group, $P<0.05. TNF: tumor necrosis factor; IL: interleukin; ELISA: enzyme-linked immunosorbent assay; BALF: bronchoalveolar lavage fluid; MAP2K3: mitogen-activated protein kinase kinase 3.

includes the anti-apoptotic factor Bcl-2 and the pro-apoptotic factor Bax. Recent studies have shown that Bcl-2 and Bax may be associated with the apoptosis of lung cells in HILI [26, 27]. During the transmission of apoptotic signals, the apoptosis is mainly induced by the activation of the caspase family members. It has been documented that the apoptotic rate of the lung epithelia increases markedly in premature newborn babies undergoing mechanical ventilation, and the caspase-3 expression is markedly activated during this process [28, 29].

In the present study, we created a neonatal rat model of HILI and measured the pathological changes in the lung tissues of both normal and HILI rats. We also examined the apoptosis of the lung tissues, the levels of Bcl-2, Bax, and caspase-3 associated with apoptosis, and the content of TNF-α and IL-6. The results revealed the presence of pulmonary cell apoptosis and the inflammatory response in the neonatal rats with HILI, which aligns with the findings of the previous studies.

miRNA is widely expressed in mammals and has become a popular fundamental research topic. Currently, studies on miRNA in HILI are few. After searching the literature, we hypothesized that miR-21-5p may have a repairing effect in HILI, as some studies reported a low level of miR-21-5p in lung alveolar epithelia during HILI [30]. Thus, we overexpressed miR-21-5p in the rat model and found that the overexpression markedly decrease the apoptosis of the lung tissues in the neonatal rats and significantly inhibited the inflammatory response, indicating that miR-21-5p can exert a good repair effect in HILI.

To further investigate the regulatory mechanism of miR-21-5p in HILI, we searched for the downstream target genes of miR-21-5p through a bioinformatics website and found the paring of MAP2K3 with miR-21-5p. MAP2K3 can participate in the oxidative stress injury in various diseases, but whether it can affect HILI remains unclear [31]. A DLR assay demonstrated that miR-21-5p can target MAP2K3. Moreover, we measured the expression levels of miR-21-5p and MAP2K3 in the lung tissues and found that miR-21-5p can negatively regulate MAP2K3 expression. After overexpressing MAP2K3 in the rat model and examining the lung cell apoptosis and the levels of the inflammatory markers, we observed that MAP2K3 overexpression can further lead to lung cell apoptosis and aggravate the inflammatory response. Com-

pared with the rats with miR-21-5p overexpression alone, the inhibitory effect of miR-21-5p overexpression on lung cell apoptosis and the inflammatory response was partially blocked in the rats with both miR-21-5p and MAP2K3 overexpression.

In conclusion, miR-21-5p overexpression can inhibit lung cell apoptosis and the inflammatory response by suppressing the expression of the downstream factor MAP2K3 in neonatal rats with HILI. However, since miRNA can regulate life activities by controlling multiple downstream target genes and because MAP2K3 overexpression cannot fully block the inhibitory effect of miR-21-5p on lung cell apoptosis and the inflammatory response, other regulatory pathways of miR-21-5p may also exist in HILI.

Acknowledgements

This work was supported by the National Natural Science Foundation of China (818-7080594), the Science & Technology Development Fund of Tianjin Education Commission for Higher Education (2019KJ200), the Youth Incubation Fund of Tianjin Medical University General Hospital (ZYYFY2015012), and the Scientific Research Funding of Tianjin Medical University Chu Hsien-I Memorial Hospital (2018ZXY02).

Disclosure of conflict of interest

None.

Address correspondence to: Yanfen Chai, Department of Emergency Medicine, Tianjin Medical University General Hospital, No. 154 Anshan Road, Heping District, Tianjin 300052, China. Tel: +86-022-60362131; Fax: +86-022-60362131; E-mail: chaiyanfentg20@163.com

References

[1] Teng RJ, Jing X, Michalkiewicz T, Afolayan AJ, Wu TJ and Konduri GG. Attenuation of endoplasmic reticulum stress by caffeine ameliorates hyperoxia-induced lung injury. Am J Physiol Lung Cell Mol Physiol 2017; 312: L586-L598.

[2] Vaidya R, Zambrano R, Hummler JK, Luo S, Duncan MR, Young K, Lau LF and Wu S. Recombinant CCN1 prevents hyperoxia-induced lung injury in neonatal rats. Pediatr Res 2017; 82: 863-871.

[3] Jing X, Huang YW, Jarzembowski J, Shi Y, Konduri GG and Teng RJ. Caffeine ameliorates hyperoxia-induced lung injury by protecting GCH1 function in neonatal rat pups. Pediatr Res 2017; 82: 483-489.

[4] Pan YQ and Hou AN. Hyperoxia-induced lung injury increases CDKN1A levels in a newborn rat model of bronchopulmonary dysplasia. Exp Lung Res 2018; 44: 424-432.

[5] Firsova AB, Bird AD, Abebe D, Ng J, Mollard R and Cole TJ. Fresh noncultured endothelial progenitor cells improve neonatal lung hyperoxia-induced alveolar injury. Stem Cells Transl Med 2017; 6: 2094-2105.

[6] Ji H, Chen M, Qian MJ, Li K, Liu GY and Qin S. Screening type II alveolar epithelial cell apoptosis related microRNA. Zhonghua Wei Zhong Bing Ji Jiu Yi Xue 2013; 25: 546-549.

[7] Song L, Zhou F, Cheng L, Hu M, He Y, Zhang B, Liao D and Xu Z. MicroRNA-34a suppresses autophagy in alveolar type ii epithelial cells in acute lung injury by inhibiting Fox03 expression. Inflammation 2017; 40: 927-936.

[8] Fang Y, Gao F, Hao J and Liu Z. microRNA-1246 mediates lipopolysaccharide-induced pulmonary endothelial cell apoptosis and acute lung injury by targeting angiotensin-converting enzyme 2. Am J Transl Res 2017; 9: 1287-1296.

[9] Lee H, Zhang D, Wu J, Otterbein LE and Jin Y. Lung epithelial cell-derived microvesicles regulate macrophage migration via microRNA-17/221-induced integrin β(1) recycling. J Immunol 2017; 199: 1453-1464.

[10] Cheng DL, Fang HX, Liang Y, Zhao Y and Shi CS. MicroRNA-34a promotes iNOS secretion from pulmonary macrophages in septic suckling rats through activating STAT3 pathway. Biomed Pharmacother 2018; 105: 1276-1282.

[11] Pan T and Xiao ZH. Expression of P38 MAPK and MMP-2 mRNA in neonatal rats with hyperoxia-induced lung injury. Zhongguo Dang Dai Er Ke Za Zhi 2013; 15: 383-386.

[12] Chang HY, Chen YC, Lin JG, Lin IH, Huang HF, Yeh CC, Chen JJ and Huang GJ. Asatone prevents acute lung injury by reducing expressions of NF-[Formula: see text]B, MAPK and inflammatory cytokines. Am J Chin Med 2018; 46: 651-671.

[13] El-Kholy AA, Elkablawy MA and El-Agamy DS. Lutein mitigates cyclophosphamide induced lung and liver injury via NF-κB/MAPK dependent mechanism. Biomed Pharmacother 2017; 92: 519-527.

[14] Dong SA, Zhang Y, Yu JB, Li XY, Gong LR, Shi J and Kang YY. Carbon monoxide attenuates lipopolysaccharide-induced lung injury by mitofusin proteins via p38 MAPK pathway. J Surg Res 2018; 228: 201-210.

[15] Lim AK, Nikolic-Paterson DJ, Ma FY, Ozols E, Thomas MC, Flavell RA, Davis RJ and Tesch GH. Role of MKK3-p38 MAPK signalling in the development of type 2 diabetes and renal injury in obese db/db mice. Diabetologia 2009; 52: 347-358.
[16] Liu Y, Shi L, Liu C, Zhu G, Li H, Zhao H and Li S. Effect of combination therapy of propofol and sevoflurane on MAP2K3 level and myocardial apoptosis induced by ischemia-reperfusion in rats. Int J Clin Exp Med 2015; 8: 6427-6435.
[17] Zhu X, Lei X, Wang J and Dong W. Protective effects of resveratrol on hyperoxia-induced lung injury in neonatal rats by alleviating apoptosis and ROS production. J Matern Fetal Neonatal Med 2020; 33: 4150-4158.
[18] Wang S, Dang H, Xu F, Deng J and Zheng X. The Wnt7b/β-catenin signaling pathway is involved in the protective action of calcitonin gene-related peptide on hyperoxia-induced lung injury in premature rats. Cell Mol Biol Lett 2018; 23: 4.
[19] Du M, Tan Y, Liu G, Liu L, Cao F, Liu J, Jiang P and Xu Y. Effects of the Notch signalling pathway on hyperoxia-induced immature brain damage in newborn mice. Neurosci Lett 2017; 653: 220-227.
[20] Endesfelder S, Weichelt U, Strauß E, Schlör A, Sifringer M, Scheuer T, Bührer C and Schmitz T. Neuroprotection by caffeine in hyperoxia-induced neonatal brain injury. Int J Mol Sci 2017; 18: 187.
[21] Donda K, Zambrano R, Moon Y, Percival J, Vaidya R, Dapaah-Siakwan F, Luo S, Duncan MR, Bao Y, Wang L, Qin L, Benny M, Young K and Wu S. Riociguat prevents hyperoxia-induced lung injury and pulmonary hypertension in neonatal rats without effects on long bone growth. PLoS One 2018; 13: e0199927.
[22] Chen CM, Hwang J, Chou HC and Shiah HS. Tn (N-acetyl-d-galactosamine-O-serine/threonine) immunization protects against hyperoxia-induced lung injury in adult mice through inhibition of the nuclear factor kappa B activity. Int Immunopharmacol 2018; 59: 261-268.
[23] Yao L, Shi Y, Zhao X, Hou A, Xing Y, Fu J and Xue X. Vitamin D attenuates hyperoxia-induced lung injury through downregulation of Toll-like receptor 4. Int J Mol Med 2017; 39: 1403-1408.
[24] Li J, Shi J, Li P, Guo X, Wang T and Liu A. Genipin attenuates hyperoxia-induced lung injury and pulmonary hypertension via targeting glycogen synthase kinase-3 β in neonatal rats. Nutrition 2019; 57: 237-244.
[25] Rudloff I, Cho SX, Bui CB, McLean C, Veldman A, Berger PJ, Nold MF and Nold-Petry CA. Refining anti-inflammatory therapy strategies for bronchopulmonary dysplasia. J Cell Mol Med 2017; 21: 1128-1138.
[26] Zhang XF and Foda HD. Pulmonary apoptosis and necrosis in hyperoxia-induced acute mouse lung injury. Zhonghua Jie He He Hu Xi Za Zhi 2004; 27: 465-468.
[27] Nyp MF, Mabry SM, Navarro A, Menden H, Perez RE, Sampath V and Ekekezie II. Lung epithelial-specific TRIP-1 overexpression maintains epithelial integrity during hyperoxia exposure. Physiol Rep 2018; 6: e13585.
[28] Yang Z, Zhang Y and Jin Z; Pediatrics DO and Hospital YU. The effect and mechanism of PGE-1 on hyperoxic lung injury in neonatal rats. J Clin Pediat 2018.
[29] Lingappan K, Maity S, Jiang W, Wang L, Couroucli X, Veith A, Zhou G, Coarfa C and Moorthy B. Role of cytochrome P450 (CYP)1A in hyperoxic lung injury: analysis of the transcriptome and proteome. Sci Rep 2017; 7: 642.
[30] Shi L, He Y, Bai B and Chen M. Effects of microRNA-21 inhibitor on apoptosis of type II alveolar epithelial cells in rats with hyperoxia-induced acute lung injury. Zhonghua Wei Zhong Bing Ji Jiu Yi Xue 2017; 29: 244-248.
[31] Lee JS and Ellis BE. Arabidopsis MAPK phosphatase 2 (MKP2) positively regulates oxidative stress tolerance and inactivates the MPK3 and MPK6 MAPKs. J Biol Chem 2007; 282: 25020-25029.